NATIONAL AERONAUTICS AND SPACE ADMINISTRATION

(NASA-CR-151056) RESULTS OF FLUTTER TEST OS6 OBTAINED USING THE 0.14-SCALE WING/ELEVON MODEL (54-0) IN THE NASA LaRC 16-FOOT TRANSONIC DYNAMICS WIND TUNNEL (Chrysler Corp.) 58 p HC A04/MF A01 N77-21177

G3/16 Unclas 24456

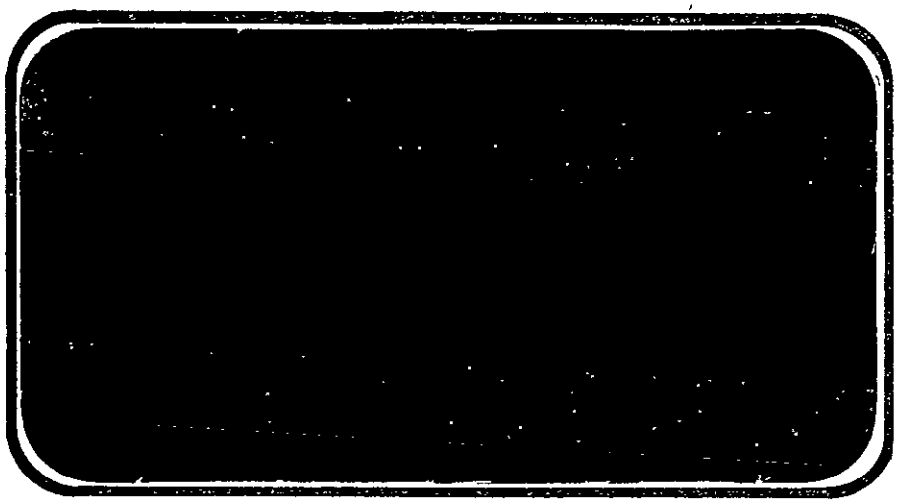

SPACE SHUTTLE

AEROTHERMODYNAMIC DATA REPORT

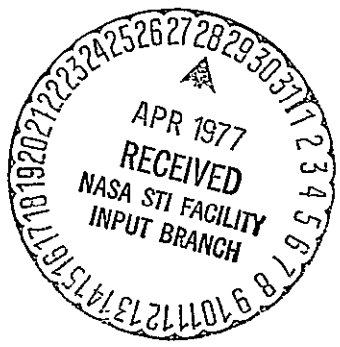

JOHNSON SPACE CENTER

HOUSTON, TEXAS

DATA MANagement services

SPACE DIVISION CHRYSLER CORPORATION

March 1977

DMS-DR-2365
NASA CR-151,056

RESULTS OF FLUTTER TEST OS6 OBTAINED USING THE 0.14-SCALE WING/ELEVON MODEL (54-0) IN THE NASA LaRC 16-FOOT TRANSONIC DYNAMICS WIND TUNNEL

by

C. L. Berthold
Shuttle Aero Sciences
Rockwell International Space Division

Prepared under NASA Contract Number NAS9-13247

by

Data Management Services
Chrysler Corporation Michoud Defense-Space Division
New Orleans, La. 70189

for

Engineering Analysis Division

Johnson Space Center
National Aeronautics and Space Administration
Houston, Texas

WIND TUNNEL TEST SPECIFICS:

Test Number:	LaRC TDT 246
NASA Series Number:	OS6
Model Number:	54-0
Test Dates:	September 3 through September 13, 1974
Occupancy Hours:	104

FACILITY COORDINATOR:

B. Spencer, Jr.
Mail Stop 365
Langley Research Center
Langley Station
Hampton, Virginia 23665

Phone: (804) 827-3911

PROJECT ENGINEERS:

C. L. Berthold
Mail Code AD38
Rockwell International
Space Division
12214 Lakewood Boulevard
Downey, California 90241

Phone: (213) 922-4620

F. Rauch
G. Commerford
T. Foley
Grumman Aerospace Corp.
Bethpage, New York 11714

Phone: (713) 488-5660

DATA MANAGEMENT SERVICES:

Prepared by: Liaison--D. A. Sarver
Operations--Maurice Moser, Jr.

Reviewed by: G. G. McDonald

Approved: J. L. Glynn, Manager
Data Operations

Concurrence: N. D. Kemp, Manager
Data Management Services

Chrysler Corporation Michoud Defense-Space Division assumes no responsibility for the data presented other than publication and distribution.

RESULTS OF FLUTTER TEST OS6 OBTAINED USING THE 0.14-SCALE WING/ELEVON MODEL (54-0) IN THE NASA LaRC 16-FOOT TRANSONIC DYNAMICS WIND TUNNEL

by

C. L. Berthold, Rockwell

ABSTRACT

A 0.14-scale dynamically scaled model of the Space Shuttle orbiter wing was tested in the Langley Research Center 16-Foot Transonic Dynamics Wind Tunnel during September 1974 to determine flutter, buffet, and elevon buzz boundaries. Mach numbers between 0.3 and 1.1 were investigated. Rockwell Shuttle model 54-0 was utilized for this investigation. A description of the test procedure, hardware, and results of this test is presented herein.

(THIS PAGE INTENTIONALLY LEFT BLANK.)

TABLE OF CONTENTS

	Page
ABSTRACT	iii
INDEX OF FIGURES	2
INTRODUCTION	3
NOMENCLATURE	4
CONFIGURATIONS INVESTIGATED	7
TEST FACILITY DESCRIPTION	13
TEST PROCEDURE	14
DATA REDUCTION	20
DISCUSSION OF RESULTS	21
REFERENCES	23
TABLES	
I. TEST SUMMARY	24
II. MODEL DIMENSIONAL DATA	25
III. CONFIGURATION DESCRIPTION AND FREQUENCY SUMMARY	29
IV. MODEL ROOT FLEXIBILITIES	30
V. PANEL MASS, INERTIA, AND C.G. VALUES	31
VI. INFLUENCE COEFFICIENTS	33
VII. MODAL ORTHOGONALITY CHECKS AND GENERALIZED MASS FOR WING WITH NOMINAL ACTUATOR STIFFNESS	34
VIII. MODAL ORTHOGONALITY CHECKS AND GENERALIZED MASS WITH REDUCED OUTBOARD ACTUATOR STIFFNESS	35
FIGURES	36

INDEX OF FIGURES

Figures	Title	Page
1.	Model installation sketch.	36
2.	Model photographs.	
	a. Rear Three-quarter View of Model Installation	37
	b. Front View of Model Installation	38
	c. Model with Fuselage Skin Removed	39
	d. Elevon Flexure Arrangement	40
3.	Model instrumentation diagram.	41
4.	Panel definition for mass and inertia measurements.	42
5.	Load points for influence coefficients.	43
6.	Flutter boundary for Configuration No. 1.	44
7.	Flutter boundary for Configuration No. 2.	45
8.	Flutter boundary for Configuration No. 3.	46
9.	True velocity versus density at Mach .6.	47
10.	True velocity versus density at Mach .649.	48
11.	True velocity versus density at Mach .7.	49
12.	True velocity versus density at Mach .8.	50
13.	True velocity versus density at Mach .85.	51
14.	True velocity versus density at Mach .90.	52
15.	True velocity versus density at Mach 1.35.	53
16.	Damping versus Mach number.	54

INTRODUCTION

Flutter boundaries for the Space Shuttle orbiter configuration 140B wing were investigated. This investigation was conducted in the NASA Langley Research Center's 16-Foot Transonic Dynamics Wind Tunnel. The model was a 0.14 scale dynamically scaled right wing panel mounted on a rigid model of a segment of the right side of the orbiter fuselage. This investigation was called OS6. The model was designed and fabricated by Grumman Aerospace Corporation under Purchase Order Agreement M3W3XMU483002 with Rockwell International Corporation's Space Division. Grumman also performed pretest measurements and calibrations of the model, conducted the test, and analyzed the test results under this same purchase order. Much of the information presented in this report was derived from Reference 1, which is Grumman's final document of its work under this purchase order.

NOMENCLATURE

SYMBOL	DEFINITION
a_r	ratio of flight vehicle to model speed of sound
CG	center of gravity
EI	bending stiffness slug - ft^3/sec^2
f	measured frequency of oscillation, Hz
F_n	Froude number
g_r	gravitational acceleration ratio
GJ	torsional stiffness, slug-ft^3/sec^2
H_o	freestream total pressure, psf
I_o	calculated moment of inertia plus tare inertia of model rig, lb-in^2
$I_{X'_{CG}}$	inertia about X' axis with origin at the center of gravity, lb-in^2
$I_{Y'_{CG}}$	inertia about Y' axis with origin at the center of gravity, lb-in^2
$I_{Z'_{CG}}$	inertia about Z' axis with origin at the center of gravity, lb-in^2
k	reduced frequency
k_r	ratio of flight vehicle to model reduced frequency
K	spring rotational rate, in-lb/radian
ℓ	geometric reference length, ft
L	length dimension
m	mass, slugs
m_r	ratio of flight vehicle to model mass
M	mass dimension
α	angle of attack, deg.

NOMENCLATURE (Continued)

SYMBOL	DEFINITION
M_∞	freestream Mach Number
P_y	load in y direction
q_∞	freestream dynamic pressure, psf
R_n	Reynolds number
T	time, sec
T_Z	torsion about Z - axis, ft-lb
v	air speed, ft/sec
W	weight, lb
X_o	orbiter longitudinal coordinate, in
X'	vertical tail coordinate perpendicular to 50% chord line, in
X'_{CG}	X' dimension of center of gravity, in
Y_o	orbiter lateral coordinate, in
Y'	vertical tail coordinate parallel to 50% chord line, in
Y'_{CG}	Y' dimension of center of gravity, in
Z_o	orbiter vertical coordinate, in
Z'	vertical tail coordinate orthogonal to vertical tail reference plane, in
Z'_{CG}	Z' of center of gravity
δ_e	elevon deflection angle, deg
δ_y	deflection in y direction, deg
θ_Z	angular deflection about Z axis, radians
H	constant total pressure

NOMENCLATURE (Concluded)

SYMBOL	DEFINITION
μ_r	ratio of model to flight vehicle absolute viscosity coefficients
ρ	freestream air density, slugs/ft^3
ω	frequency, h_z
$\mathcal{H}$	hinge line
$\mathcal{C}$	center line

SUBSCRIPTS

SYMBOL	DEFINITION
a/c	full scale flight vehicle value
model	model value
r	ratio of model to flight vehicle
X	value referenced to X - axis
X'	value referenced to X' - axis
Y	value referenced to Y - axis
Y'	value referenced to Y' - axis
Z	value referenced to Z - axis
Z'	value referenced to Z' - axis

CONFIGURATIONS INVESTIGATED

The wing-elevon model was a 0.140 geometric scale representation of 140B Space Shuttle Orbiter components. It was dynamically scaled; i.e., the reduced frequency ratio and mass density ratio were scaled to 1.0 to properly simulate stiffness and mass properties of the full scale structures. The model scale factors were established to assure that estimated flutter boundaries fall within the range of the LaRC 16-foot TDT. The model had a stressed skin design constructed of epoxy-resin (pre-preg) fiberglass plies layed up on cellular-cellulose acetate (CCA) foam backing; local areas such as root attachments and actuator back up structure were reinforced by steel sheet (.003" thick) to assure a smooth load transition at the metal-fiberglass interfaces. The model had a control surface (elevon) with actuator stiffnesses modeled by steel flexural pivots. Access panels at the control surface actuator locations facilitated changing the pivot flexures. Different flexures were tested to simulate nominal, 75% of nominal, and 50% of nominal actuator stiffnesses. Fuselage fairings adjacent to the wing were size scaled to simulate proper local flow characteristics as well as to place the surfaces outside the tunnel boundary layer; they were not dynamically scaled. The fairings were constructed of fiberglass skin attached to aluminum frames. The model consisted of the following components:

1. One sidewall mount to tunnel mounting plate
2. One partial non-dynamic fuselage

3. One wing assembly (including elevons)
4. One additional set elevons (inboard and outboard)
5. Nine elevon flexure sets:
   (a) 3 Stiffness Level 1
   (b) 3 Stiffness Level 2
   (c) 3 Stiffness Level 3
6. One internal model shaker
7. One control surface deflect/release mechanism per elevon
8. Eight (8) strain gage circuits (4 bending, 4 torsion)
9. Two magnetic induction coil elevon position indicators
10. One accelerometer (wing tip)
11. Control panel for shaker and deflect/release mechanism

Note: Items 6 through 10 and one (1) set of item 5 are included in Item 3.

Figure 1 shows a sketch of the model assembly and Figure 2 presents photographs of the model.

The following scaling parameters were used to simulate an altitude of 30,000 feet during the test:

CONFIGURATIONS INVESTIGATED (Continued)

PARAMETER	SYMBOL	DIMENSIONS	EQUATION	VALUE
Length	ℓ	L	$\ell_r=\ell_{model}/\ell_{a/c}$	.14
Air Density	ρ	ML^{-3}	$\rho_r=\rho_{model}/\rho_{a/c}$	1.07
Air Speed (1)	v	LT^{-1}	$v_r=v_{model}/v_{a/c}$	.52
Dynamic Pressure	q	$ML^{-1}T^{-2}$	$\rho_r v_r^2$	.292
Frequency	ω	T^{-1}	$k_r v_r/\ell_r/\mu_r$	3.73
Velocity (1)		LT^{-1}	$k_r v_r$	.52
Acceleration		LT^{-2}	$k_r^2 v_r^2/\ell_r$	1.95
Mass	m	M	$\mu_r\rho_r\ell_r^3$	2.93×10^{-3}
Mass Unbalance		ML	$\mu_r\rho_r\ell_r^4$	4.11×10^{-4}
Mass Moment of Inertia		ML^2	$\mu_r\rho_r\ell_r^5$	5.75×10^{-5}
Stiffness	EI,GJ	ML^3T^{-2}	$k_r^2 v_r^2\rho_r\ell_r^4$	1.11×10^{-4}
Bending Spring Constant		MT^{-2}	$k_r^2 v_r^2\rho_r\ell_r$	4.09×10^{-2}
Torsional Spring Constant		ML^2T^{-2}	$k_r^2 v_r^2\rho_r\ell_r^3$	8.01×10^{-4}
Force		MLT^{-2}	$k_r^2 v_r^2\rho_r\ell_r^2$	5.72×10^{-3}
Moment		ML^2T^{-2}	$k_r^2 v_r^2\rho_r\ell_r^3$	8.01×10^{-4}
Mass Density Ratio	μ	———	$\mu_r=m_r/\rho_r\ell_r^3$	1.0
Reduced Frequency	k	———	$k_r=\ell_r\omega_r/v_r$	1.0
Froude Number	F_n	———	$k_r^2 v_r^2/\ell_r g_r$	1.93
Reynolds Number	R_n	———	$\rho_r v_r \ell_r/\mu_r^*$	.087
Mach Number	M	———	v_r/a_r	1.0

Where: μ_r^* = absolute viscosity coefficient ratio = .90

g_r = gravitational acceleration ratio = 1.0

a_r = sonic speed ratio = .52

Air speed is the aircraft flight speed; velocity is the speed associated with vibrations of the model. These quantities differ only when the reduced frequency ratio is not unity.

The following nomenclature was used to designate the model components:

B_{26}	Body	Similar to B_{26} lines in area of wing. Only left-hand side duplicated outboard of B.L. 63 and with truncated forward fuselage section.
M_7	OMS Pod	Outboard portion, left-hand side only.
W_{128}	Wing	Left-hand wing only similar to W_{116} except modified to remove spanwise twist from airfoil section
B_{45}	Elevons	Inboard and outboard left side only.

A complete description of model components and dimensional data is given in Table II. The model was referred to as configuration 1, 2, or 3 depending on which flexures were used for the elevon. Table III defines these configurations.

The model was equipped with its own internal shaker and control surface deflector/release mechanism; this device was remotely activated in the tunnel control room by a GAC supplied control box. The shakers were of the rotary unbalanced force type driven by a flexible cable shaft and designed to produce an approximately constant force output (1.5 to 2 lbs.) from 15 to 70 Hz. The model control surface deflector/release mechanism consists of a roller cam, mounted on a pivot arm attached to the aft face of the main surface rear spar, which contacts a pawl attached to the front face of the control surface front spar. To deflect and release, i.e., "pluck" the control surface, the pivot arm

was rotated via an attached cable until the roller cam contacted the pawl, forcing it aside. This action deflected the control surface until the cam overrode the pawl, releasing the control surface.

The model had the following instrumentation:

Type of Measurement	Device Used
Uncalib. Wing Bending Moment	Four active arm strain gage circuits
Uncalib. Wing Torsion	
Uncalib. Wing Bending Moment	
Uncalib. Wing Torsion	
Uncalib. Dynamic Elevon Position (inboard)	Magnet & coil assembly
Uncalib. Dynamic Elevon Position (outboard)	
Wing Tip Acceleration	Endevco 2264 accelerometer
Inboard Elevon Hinge Moment	Tension link
Outboard Elevon Hinge Moment	
Excitation Frequency	Motor tachometer

Figure 3 diagrams the instrumentation setup.

TEST FACILITY DESCRIPTION

Major elements of the NASA Langley Transonic Dynamics Tunnel are an electric motor drive system, a cooling system, a gas-handling system, a tunnel control room and observation chamber, a transonic test section, and a model calibration laboratory.

Test section is 16 feet square and has a uniform flow region more than 10 feet in length. Throughout this region, Mach number deviation is less than $\pm$ .005 for subsonic speeds and generally less than $\pm$ .01 above Mach 1. Maximum Mach number is 1.20. Mach number, which depends on compression ratio across the fan, is controlled by varying the motor rpm or remotely varying the angle of pre-rotation located ahead of the fan.

Transonic flow is generated by three slots in both the ceiling and floor of the test section.

Drive system consists of a two-speed range wound-rotor induction motor directly connected to a fan which may be considered as a single-stage compressor. Fan speed ranges are 24 to 235 rpm for operation in Freon-12 and 15 to 470 rpm for operation in air.

Motor speed is automatically controlled by a liquid rheostat and eddy current brake to better than $\pm$ ¼ percent. At the maximum rpm in each speed range, shaft output is 20,000 horsepower, continuous rating.

Cooling system consists of a two-row vertical tube cooler through which water is circulated to maintain a stagnation temperature under 150°F.

TEST PROCEDURE

Various calibrations and measurements were performed on the model prior to the test to determine its dynamic properties. These are described below:

Flexibility influence coefficients were measured and compared to the scaled full scale coefficients.

Influence coefficients were measured as the deformation slopes (spanwise and chordwise) per unit load due to force loads singly applied to the models at prescribed locations. The slopes were measured with small mirrors attached parallel to a model surface at prescribed locations. The mirrors reflected a projected grid network onto a vertically oriented screen; any change in the angular position (slope) of a mirror due to a change in loading was detected and measured on the screen. For these measurements, the vertically oriented models were cantilevered from their respective root attachment fittings, which simulate fuselage flexibility, and the loads were applied with weight and pulley arrangements. Separate measurements of the model root attachment fitting flexibilities were made with the respective model detached; the influence coefficients (flexibilities) were the root attachment spring displacements per unit load at the point of load application. Again, the loads were applied with weights, but the linear displacements (Y and Z directions) were measured with a linear differential transformer. Resulting root flexibilities are presented in Table IV. Resulting influence coefficients are presented in Table VI.

Figure 5 shows the load points used to determine influence coefficients.

Model mass distribution was also scaled in addition to stiffness scaling for complete model dynamic simulation. To demonstrate compliance with the required model mass distribution, the following inertial properties of the model were measured:

1. weights of main surfaces and control surfaces
2. C.G. locations of the main and control surface structures
3. moments of inertia of the main surfaces about their C.G. X, Y, and Z axes
4. hinge line inertias for the control surfaces
5. C.G. moments of inertia of complete models about the pitch (Y) axis for the wing and yaw (Z) axis for the fin

The center of gravity of each model component (main and control surfaces) were located by suspending the model alternately at several (at least two) pivot points, scribing the plumb lines from the pivot points on the model surface, and thereby determining the C.G. as the intersection of these lines. Model moments of inertia were measured with the aid of a low frequency vibration rig, which was essentially an oversized flexural pivot, or a bifilar pendulum,depending on the reference axis. When using the vibration rig, the model was cantilevered normal to one of the flexural pads and caused to oscillate freely about the flexural axis. The frequency of oscillation was measured with an accelerometer mounted on the moving flexural pad. The moment of inertia of the model and the tare inertia of the rig about its flexural axis is determined from the

following relationship:

$$I_o = K/(2\pi f)^2,$$

where:

K was the measured rotational spring rate of the rig about its flexural axis (inch pounds/radian),

f was the measured frequency of oscillation (Hz), and

I_o was the calculated moment of inertia of the model plus the tare inertia of the rig about its flexural axis.

It was a simple matter to subtract the known tare inertia of the rig from the calculated inertia, I_o and transfer the resultant model inertia about the flexural axis to the model's C.G. axis to obtain the model C.G. moment of inertia. The pitch axis moment of inertia was measured using a bifilar pendulum to measure oscillatory frequencies instead of the vibration rig because of model mounting constraints. These calculations were done on a panel by panel basis with panels as shown on Figure 4. Resulting calculations and measurements are given in Table V.

Measured model modes and frequencies were compared to calculated full-scale modes and frequencies (assuming correct model/full scale weight ratio). Ground vibration surveys were conducted on the model cantilevered from its fuselage root attachment springs. The model was instrumented with one fixed and one survey (movable) accelerometer (Endevco - Model 2264-150). Vibration excitation was provided by an electromechanical shaker with a lightweight movable element secured to the model (Miller Model-A6466). During the vibration survey, while

monitoring the response of the fixed reference accelerometer on an oscilloscope, a frequency sweep was made and the large amplitude resonant responses were noted for the first five modes of each model; then returning to the first noted resonant response and dwelling there, a survey of the structural response was made with the portable accelerometer moved to prescribed locations on the wing model for each successive mode. Generalized mass of the modes was determined experimentally by the procedure outlined in reference 2 and is presented in tables VII and VIII. Additional measurements were made during the test period using a hand held probe for data acquisition and a Goodman electromagnetic shaker for excitation. These measurements are documented in reference 1.

The model was proof-loaded to assure it possessed adequate strength to sustain the inertial and aerodynamic loads acting on it during the wind tunnel testing. The proof loads were based on a load estimate schedule prescribed by Rockwell International. The model test loadings were achieved by placing lead sheets on the model's surface to yield equivalent shear loads and bending moments at the roots.

The wing model was mounted in the Langley Research Center 16-foot Transonic Dynamic Tunnel cantilevered off the east side wall with the fuselage fairing and root attachment fitting. Within the model fuselage fairing was a rigid framed support structure which also acted as a mounting butt for the model on its root attachment fitting; the structure was bolted to the tunnel sidewall turntable; this turntable varied the model

angle of attack. The shaker flexible drive cable, control surface deflector/release cable, strain gage, control surface coil, accelerometer and force link wiring were rooted from the semi-span mount through to the control room via stainless steel tubing. Figure 1 presents a sketch of the model installation. Figure 3 presents photographs of the installation.

The general operating procedure was to make progressively higher constant total pressure sweeps through the Mach range from 0.6 to 1.2 until the ascent trajectory plus the required 32% margin of safety was investigated. Following this, testing continued at more extreme operating conditions until flutter was obtained or tunnel operating limits were reached. Pauses were made at several discrete Mach nos. during each sweep to stabilize tunnel conditions. At these points, the main model surfaces and control surfaces were excited, respectively, by the internally mounted rotary unbalanced shaker and control surface deflect/release mechanisms. During shaker excitation, the measured model amplitudes and frequencies were recorded and interpreted to assist in predicting the onset of flutter. After the shaker excitation, each control surface was deflected and released in an attempt to initiate "buzz." During the deflect/release operation, the control surface hinge moment was measured in an attempt to predict the onset of "buzz." This procedure was done as follows:

1. The model was installed and visually inspected in the tunnel;

2. Modal frequencies were checked with the aid of an electro-mechanical shaker and the model instrumentation;

3. The desired tunnel operating path was selected;

4. The wind-off data readouts were recorded;

5. The wind tunnel was started and the model was trimmed to zero lift during the first low q run;

6. Desired Mach number and dynamic pressure were obtained;

7. When flow conditions stabilized, the model shaker was operated at a constant sweep rate from 15-70 H_z. At the conclusion of the sweep, a review of the data was made (plots of 1/modal amplitude and modal frequency vs. q were made and used to predict the onset of flutter);

8. If no flutter was observed during step 7, the control surfaces were "plucked" one at a time in an attempt to initiate control surface "buzz"; during this "plucking" operation, a record was made of the control surface hinge moment via the force link in the actuator cable of the plucker device;

9. If no flutter was observed during step 8, a higher Mach number and q on the same constant total pressure path was used to repeat steps 7 and 8;

10. Steps 4 through 9 were repeated for different values of constant total pressure (H) until the Orbiter ascent trajectory boundary was cleared and/or the flutter boundary defined in the transonic flight regime;

11. Steps 2 - 10 were repeated for each new control surface configuration.

Two high speed movie cameras and a T.V. monitor were used during the runs to record any dynamic instability. The movie cameras were located to provide both a side view and rear view of the model.

Table I summarizes the test program and tunnel conditions.

DATA REDUCTION

Freestream data were measured and reduced using standard test facility techniques. Model data recorded were:

1. Oscillograph traces of the model strain gage circuits.
2. Oscillograph traces of tunnel parameters.
3. High speed movies.
4. Tabulated data.

Figures 6 through 16 present plots of the test results.

DISCUSSION OF RESULTS

Tests on the wing were made to investigate the effect of varying the stiffness of the outboard elevon actuator on the dynamic characteristics of the wing model. To achieve this goal, a series of three configurations were tested. Table III outlines a description of the various configurations tested and a summary of the frequencies measured on those configurations with the model installed in the tunnel. Due to the large amount of camber in the wing, a series of runs was made to establish minimum load conditions on the model. The model mount was designed so that small changes in the angle of attack of the fuselage, and thus the wing, could be made remotely. Table I, in addition to summarizing the maximum tunnel conditions, lists the angles of attack and elevon deflection angles required to minimize model loads.

Configuration No. 1 was made with nominal elevon actuator stiffness. Although runs 31 through 47 were made in this configuration, only runs 41 through 47 were made at sufficiently high dynamic pressure to clear the configuration. The other runs were mainly used to establish model trim conditions. No flutter or other dynamic instability was encountered within the tested region. A summary plot of test conditions may be found in Figure 6.

Runs 48 through 53 were made with the model in configuration 2. During these runs flutter was not encountered; however, some low damping was noted during runs 51, 52, and 53. A plot of test conditions for configuration No. 2 may be found in Figure 7.

For configuration No. 3, the outboard elevon actuator stiffness was reduced below the level tested during configuration 2. Runs 54 through 57 were made in this configuration and flutter was encountered during run 57, which resulted in loss of the outboard elevon. The flutter frequency was recorded at 28 Hz indicating, along with visual observation, that the flutter mechanism involved the outboard elevon rotation and wing 1st bending modes. See Figure 8 for a plot of test conditions for configuration No. 3.

The following observations were made:

1. No flutter was detected on the wing model with nominal elevon actuator stiffness within the scaled trajectory.

2. Flutter was encountered with the wing model when the stiffness of the simulated outboard elevon actuator was significantly reduced.

REFERENCES

1. F. Rauch and T. Foley, "Results of Dynamic Tests and Flutter Analyses Performed on .14 Scale Models of the Shuttle Wing and Fin," Grumman Aerospace Report No. LD-RS-11, November 18, 1974.

2. Manual on Aeroelasticity, Volume IV, AGARD.

3. C. L. Berthold, "Pretest Information for Component SSV Flutter Tests of 0.14-Scale Wing-Elevon (54-0) and Fin-Rudder (55-0) Models in the NASA-LRC 16-Foot Transonic Dynamics Tunnel (Tests OS6 and OS7)," Rockwell International Report SD74-SH-0148, July 5, 1974.

4. Langley Working Paper (LWP-799) The Langley Transonic Dynamics Tunnel, September 23, 1969.

5. Drawings:

Drawing No.	Description
SS-S-00151	General Arrangement and Assembly
SS-S-00152	Installation LRC TDT (54-0 and 55-0)
SS-S-00153 (1-5)	Skin Definition - Wing
SS-S-00156	Fuselage Assembly
SS-S-00157	Fuselage Frame Assembly
SS-S-00158	Fuselage Shell
SS-S-00161	Shaker Assembly and Detail
SS-S-00162 (1&2)	Wing Fittings and Flexures
SS-S-00163	Root Fittings
SS-S-00169	Hinge Fittings at WS 147.5 and 435
SS-S-00170	Flexure and Fittings, Sta. 212
SS-S-00171	Hinge Fittings at WS 282 and 342.5
SS-S-00172	Loading Tube - Checkout
SS-S-00173	Flexure and Fittings at WS 387.5
SS-S-00174	Ballast Supports
SS-S-00175 (1-2)	Elevon Actuator Details
SS-S-00176	Shaker Springs

TABLE I. TEST SUMMARY

RUN NO.	CONFIGURATION NO.	FLEXURE THICKNESS (IN) INBOARD ELEVON	FLEXURE THICKNESS (IN) OUTBOARD ELEVON	α (DEG)	δ_e DEG.	MACH NO.	DYNAMIC PRESSURE (PSF)	DENSITY (SLUGS) /ft^3	VELOCITY (FT/SEC)	TOTAL PRESSURE (PSF)	REMARKS
31	1	0.300	0.228	0 to -2	0	.431	29.6	0.00125	217.2	300	Trim Run
32	↓	↓	↓	--	↓	--	--	---	--	300	Trim Run
33				-1.1		1.101	87.4	0.00059	545.4	200	High Elevon Down
34				↓		0.908	168.7	0.00162	455.8	500	Load
35						0.766	212.0	0.00283	385.7	800	↓
36						0.608	218.9	0.00461	306.4	1200	
37				0 to -2		0.829	120.2	0.00139	414.8	400	Trim Run
38				-1.0	3	1.061	167.8	0.00118	532.3	400	High Wing Lift
39				-1.0	3	0.762	179.5	0.00240	385.3	700	↓
40				-2.2	6	1.099	129.0	0.00086	548.2	300	Trim Run
41				-5		1.103	172.9	0.00114	550.6	400	Moderate Loads
42						0.800	221.8	0.00272	402.2	800	Slight Damage to Hatch
43						0.886	260.9	0.00262	445.1	800	
44						0.750	280.5	0.00395	378.4	1200	
45						0.655	302.7	0.00545	331.2	1500	
46						0.600	318.1	0.00690	301.2	1800	
47				-4		1.054	295.9	0.00208	531.4	450 to 850	
48	2		0.181	-5		0.950	144.3	0.00129	472.1	400	
49			↓			0.907	227.6	0.00221	453.0	700	
50						0.901	291.1	0.00283	452.3	900	
51						0.731	290.0	0.00426	367.7	1200	
52						0.695	318.4	0.00514	349.8	1400	
53						0.721	386.7	0.00581	362.5	1600	
54	3		1 @ .181 1 @ .125			0.907	128.7	0.00125	453.5	400	
55						0.909	227.2	0.00217	455.7	700	
56						0.906	292.3	0.00297	406.5	900	
57		↓	↓	↓	↓	0.649	238.2	0.00447	324.9	1200	Outboard Elevon Fluttered and Detached

TABLE II. MODEL DIMENSIONAL DATA

MODEL COMPONENT: BODY - B_{26}

GENERAL DESCRIPTION: Configuration 140A/B orbiter fuselage

NOTE: B_{26} is identical to B_{24} except underside of fuselage has been refaired to accept W_{116}

MODEL SCALE: 0.140 MODEL DRAWING: SS-A00147, Release 12

DRAWING NUMBER: VL70-000143B, -000200, -000205, 006089, -000145
VL70-000140A, -000140B

DIMENSIONS	FULL SCALE	MODEL SCALE
Length (OML: Fwd Sta. X_o = 235), in.	1293.3	181.062
Length (IML: Fwd Sta. X_o = 238), in.	1290.3	180.642
Max Width (@ X_o = 1528.3), in.	264.00	36.96
Max Depth (@ X = 1464), in.	250.00	35.00
Fineness Ratio	0.26357	0.26357
Area - Ft^2		
Max. Cross-Sectional	340.88	6.68

TABLE II. MODEL DIMENSIONAL DATA (Continued)

MODEL COMPONENT: ELEVON - E_{45}

GENERAL DESCRIPTION: Elevon for configuration 140C/D, hingeline at X_o = 1387, elevon split line relocated from Y_o - 281 to Y_o = 312.5

MODEL SCALE: 0.140

DRAWING NUMBER: VL70-000140C, -000200B, -006089, -006092

DIMENSIONS:	FULL SCALE	MODEL SCALE
Area, Ft^2	210.0	4.116
Span (equivalent), In.	349.2	48.888
Inb'd equivalent chord, In.	118.0	16.520
Outb'd equivalent chord, In.	55.19	7.727
Ratio movable surface chord/ total surface chord		
At Inb'd equiv. chord	0.2096	0.2096
At Outb'd equiv. chord	0.4004	0.4004
Sweep Back Angles, degrees		
Leading Edge	0.00	0.00
Trailing Edge	- 10.056	- 10.056
Hingeline	0.00	0.00
Area Moment (Product of area and $\bar{c}$), Ft^3	1587.25	4.36
Mean Aerodynamic Chord, In.	90.7	12.698

TABLE II. MODEL DIMENSIONAL DATA (Continued)

MODEL COMPONENT: OMS/RCS PODS - M_7

GENERAL DESCRIPTION: Configuration 140A/B Orbiter OMS/RCS pods.

MODEL SCALE: 0.140 **MODEL DRAWING:** SS-A00147, Release 12

DRAWING NUMBER: VL70-000145

DIMENSIONS:	FULL SCALE	MODEL SCALE
Length (OMS Fwd Sta X_o = 1233.0), in.	327.000	45.78
Max Width (@ X_o = 1450.0), in.	94.500	13.230
Max Depth (@ X_o = 1493), in.	109.000	15.25

TABLE II. MODEL DIMENSIONAL DATA (Concluded)

MODEL COMPONENT: WING - W_{128}

GENERAL DESCRIPTION: Configuration 4

NOTE: Identical to W_{114} and W_{116} except modified to remove spanwise twist from airfoil section.

MODEL SCALE: 0.140 DRAWING NO.: VL70-000140A, -000200

DIMENSIONS:	FULL SCALE	MODEL SCALE
TOTAL DATA		
Area (Theo.), ft^2		
Planform	2690.00	52.724
Span (Theo.), in.	936.68	131.135
Aspect Ratio	2.265	2.265
Rate of Taper	1.177	1.177
Taper Ratio	0.200	0.200
Dihedral Angle, degrees	3.500	3.500
Incidence Angle, degrees	0.500	0.500
Aerodynamic Twist, degrees	+ 3.000	0.000
Sweep Back Angles, degrees		
Leading Edge	45.000	45.000
Trailing Edge	- 10.056	- 10.056
0.25 Element Line	35.209	35.209
Chords:		
Root (Theo.) B.P.0.0.	689.24	96.494
Tip, (Theo.) B.P.	137.85	19.299
MAC	474.81	66.473
Fus. Sta. of .25 MAC	1136.83	159.156
W.P. of .25 MAC	290.58	40.681
B.L. of .25 MAC	182.13	25.498
EXPOSED DATA		
Area (Theo.), ft^2	1751.50	34.33
Span, (Theo.), in. BP108	720.68	100.895
Aspect Ratio	2.059	2.059
Taper Ratio	0.245	0.245
Chords		
Root BP108	562.09	78.693
Tip 1.00 b/2	137.85	19.299
MAC	392.83	54.996
Fus. Sta. of .25 MAC	1185.98	166.037
W.P. of .25 MAC	294.30	41.202
B.L. of .25 MAC	251.77	35.248
Airfoil Section (Rockwell Mod NASA) XXXX-64		
Root b/2 =	0.113	0.113
Tip b/2 =	0.120	0.120
Data for (1) of (2) Sides		
Leading Edge Cuff		
Planform Area, ft^2	113.18	2.218
Leading Edge Intersects Fus M.L. @ Sta	500.00	70.00
Leading Edge Intersects Wing @ Sta	1024.00	143.36

TABLE III. CONFIGURATION DESCRIPTION AND FREQUENCY SUMMARY

CONF. NO.	CONFIGURATION DESCRIPTION	MEASURED FREQUENCIES = HZ				
		1	2	3	4	5
1	4 inboard flexures - thickness = .300, width = .60 2 outb'd flexures - thickness = .228, width = .35 (nominal actuator stiffness)	21.05	35.0	42.0	48.0	57.0
1a	3 inboard flexures - thickness = .300, width = .60 1 inboard flexure - thickness = .210, width = .60 2 outb'd flexures - thickness = .228, width = .35	21.05	35.0	42.0	48.0	57.0
2	3 inboard flexures - thickness = .300, width = .60 1 inboard flexure - thickness = .210, width = .60 1 outb'd flexure - thickness = .181, width = .35 1 outb'd flexure - thickness = .181, width = .25	20.70	33.01	36.83	44.94	55.04
3	3 inboard flexures - thickness = .300, width = .60 1 inboard flexure - thickness = .210, width = .60 1 outb'd flexure - thickness = .181, width = .35 1 outb'd flexure - thickness = .125, width = .35	19.65	31.87	35.88	44.67	55.25

NOTE: Flexures are made of steel and are configured as 90° cross-flexures.

TABLE IV. MODEL ROOT FLEXIBILITIES

"Y" AXIS

LOCATION		DESIGN VALUE - IN/LB (MODEL SCALE)	MEASURED VALUE - IN/LB (MODEL SCALE	MEAS. DESIGN
807	lower	* 0.611×10^{-4}	0.674×10^{-4}	1.10
	upper	*453.0×10^{-4}	370.0×10^{-4}	.82
919	lower	0.440×10^{-4}	0.464×10^{-4}	1.05
	upper	3.081×10^{-4}	2.85×10^{-4}	.93
1009.75	lower	0.660×10^{-4}	0.643×10^{-4}	.97
1040	lower	0.318×10^{-4}	0.294×10^{-4}	.92
	upper	1.980×10^{-4}	1.870×10^{-4}	.94
1123	upper	**396.1×10^{-4}	322×10^{-4}	.81
1191	lower	0.318×10^{-4}	0.308×10^{-4}	.97
	upper	0.538×10^{-4}	0.536×10^{-4}	1.0
1249	lower	0.245×10^{-4}	0.250×10^{-4}	.98
	upper	0.269×10^{-4}	0.266×10^{-4}	.99
1307	lower	0.171×10^{-4}	0.174×10^{-4}	1.02
	upper	0.245×10^{-4}	0.239×10^{-4}	.98
1365	lower	0.269×10^{-4}	0.294×10^{-4}	1.09
	upper	0.367×10^{-4}	0.375×10^{-4}	1.02

"Z AXIS

807.0	* 11.10 x 10	10.54×10^{-4}	.95
919.0	9.58×10^{-4}	8.33×10^{-4}	.87
1009.75	2.03×10^{-4}	1.37×10^{-4}	.67
1040.0	7.14×10^{-4}	5.70×10^{-4}	.80
1123.0	** 1.30×10^{-4}	1.61×10^{-4}	1.24
1191.0	4.06×10^{-4}	4.05×10^{-4}	1.00
1249.0	3.08×10^{-4}	3.11×10^{-4}	1.01
1307.0	1.71×10^{-4}	1.78×10^{-4}	1.04
1365.0	2.10×10^{-4}	2.23×10^{-4}	1.06

* Value for X = 835 used for X = 807

** Value for X = 1115.5 used for X = 1123

TABLE V. PANEL MASS, INERTIA, AND C.G. VALUES

CALCULATED VALUE FOR WING WITHOUT ELEVONS							
PANEL	W (LBS)	X_{CG} (IN)	Y_{CG} (IN)	PANEL	W (LBS)	X_{CG} (IN)	Y_{CG} (IN)
1	1.46	14.45	2.73	26	0.12	80.28	22.82
2	6.59	42.22	2.58	28	0.34	49.78	27.02
3	1.67	65.69	2.06	29	1.26	66.05	26.57
4	0.10	80.32	3.32	30	0.17	79.70	26.89
6	1.12	15.02	6.82	32	0.13	51.65	31.15
7	4.38	41.87	7.31	33	1.21	65.76	30.72
8	1.65	66.28	6.68	34	0.13	80.28	31.09
9	0.20	79.63	6.23	36	1.14	66.15	34.85
11	0.17	24.15	11.07	37	0.20	80.26	35.29
12	0.90	39.77	11.34	39	1.86	72.52	39.52
13	1.17	65.80	10.84	40	0.40	78.82	39.54
14	0.11	80.33	11.20	42	0.73	69.36	43.04
16	0.91	42.42	15.20	43	0.12	80.22	43.54
17	1.87	69.86	14.78	45	0.38	71.36	46.27
18	0.44	78.68	14.97	46	0.06	79.46	46.96
20	0.73	44.93	19.01	48	0.07	74.41	49.78
21	1.27	65.77	18.58	49	0.02	79.46	49.78
22	0.12	80.28	18.90				
24	0.56	48.45	23.14	TOTAL CALCULATED	34.924	53.77	14.93
25	1.25	66.08	22.60				

	CALCULATED AND MEASURED VALUES FOR WING WITH ELEVONS					
	W (LBS)	X_{CG} (IN)	Y_{CG} (IN)	$I_{XX_{CG}}$ (LB-IN^2)	$I_{YY_{CG}}$ (LB-IN^2)	$I_{ZZ_{CG}}$ (LB-IN^2)
CALCULATED	41.17	171.70	31.14	9,917	20,611	29,521
MEASURED	42.53	172.47	31.65	9,134	22,565	30.467

NOTE: See Figure 4 for definition of panels

X_{CG} is distance aft of orbiter station 807.0

Y_{CG} is distance outb'd of orbiter station 105.0

TABLE V. PANEL MASS, INERTIA, AND C.G. VALUES (Concluded)

INBOARD ELEVON					
PANEL	W (LBS)	X_{CG} (IN)	Y_{CG} (IN)	I_{YCG} (LB-IN^2)	I_{HL} (LB-IN^2)
5	0.45	85.74	3.89	3.68	12.91
10	0.67	86.98	6.43	20.43	42.71
15	0.50	87.40	11.19	10.68	29.92
19	0.54	86.51	14.88	11.12	26.36
23	0.48	87.54	18.82	9.10	28.45
27	0.46	87.51	22.44	7.80	26.33
31	0.57	87.95	26.80	9.38	35.35
TOTAL CALCULATED	3.67	87.11	14.83	73.85	202.03
TOTAL MEASURED	3.52	86.86	15.02	70.92	208.95

OUTBOARD ELEVON					
PANEL	W (LBS)	X_{CG} (IN)	Y_{CG} (IN)	I_{YCG} (LB-IN^2)	I_{HL} (LB-IN^2)
35	0.56	85.55	31.26	6.01	16.72
38	0.55	85.57	35.56	5.41	15.95
41	0.50	83.09	38.29	4.22	6.01
44	0.49	85.65	43.92	3.11	12.85
47	0.26	86.34	46.69	1.13	7.74
50	0.22	85.93	49.59	0.70	5.60
TOTAL CALCULATED	2.58	85.20	39.03	23.51	64.87
TOTAL MEASURED	2.59	85.30	39.03	24.23	61.77

NOTE: See Figure 4 for definition of panels

TABLE VI. INFLUENCE COEFFICIENTS

UNIT LOAD POINTS	DEFLECTIONS DUE TO UNIT LOADS X 10^{-4}														
	1	2	3	4	5	6	7	8	9	10	11	12	13	14	
1	4.40	1.10		1.40			.50				0				M
	5.40	3.13		2.22			1.99				.98				D
2		3.40		1.90			1.10				1.00				M
		3.57		2.40			1.69				1.32				D
3			6.70		5.30			4.40				3.80			M
			8.92		6.31			4.99				4.03			D
4				3.20			1.40				1.40				M
				3.20			2.05				1.76				D
5					7.40			4.80				5.30			M
					7.24			5.75				5.21			D
6						11.30			10.80				10.00		M
						13.40			11.00				10.05		D
7							3.20				2.40				M
							3.03				2.54				D
8								7.80				7.20			M
								7.60				7.11			D
9									13.80				14.20		M
									13.45				13.30		D
10										20.80				21.10	M
										23.08				22.67	D
11											3.80				M
											4.65				D
12												11.30			M
												10.32			D
13													17.40		M
													17.73		D
14														29.35	M
														32.27	D

NOTE: M = Measured Value
D = Designed Value
See Figure 5 for definition of load points

TABLE VII. MODAL ORTHOGONALITY CHECKS AND GENERALIZED MASS WITH REDUCED OUTBOARD ACTUATOR STIFFNESS

MODE	1	2	3	4	5
1	1.000	.0036	.0041	.0058	.00002
2	———	1.000	.0022	.0013	.0080
3	———	———	1.000	.0173	.0123
4	———	———	———	1.000	.0041
5	———	———	———	———	1.000
FREQ. (HZ)	21.39	35.46	41.46	47.11	56.40
GENERALIZED MASS					
CALCULATED	3.223	1.113	0.835	1.165	1.569
MEASURED	3.214	1.047	1.335	1.180	1.606

TABLE VIII. MODAL ORTHOGONALITY CHECKS AND GENERALIZED MASS WITH REDUCED OUTBOARD ACTUATOR STIFFNESS

MODE	1	2	3	4	5
1	1.000	.0087	.0078	.00004	.0175
2	———	1.000	.0025	.0312	.0003
3	———	———	1.000	.0100	.0354
4	———	———	———	1.000	.0150
5	———	———	———	———	1.000
FREQUENCY (HZ)	19.65	31.87	35.88	44.67	55.25
GENERALIZED MASS CALCULATED	4.343	1.914	1.786	1.173	1.381

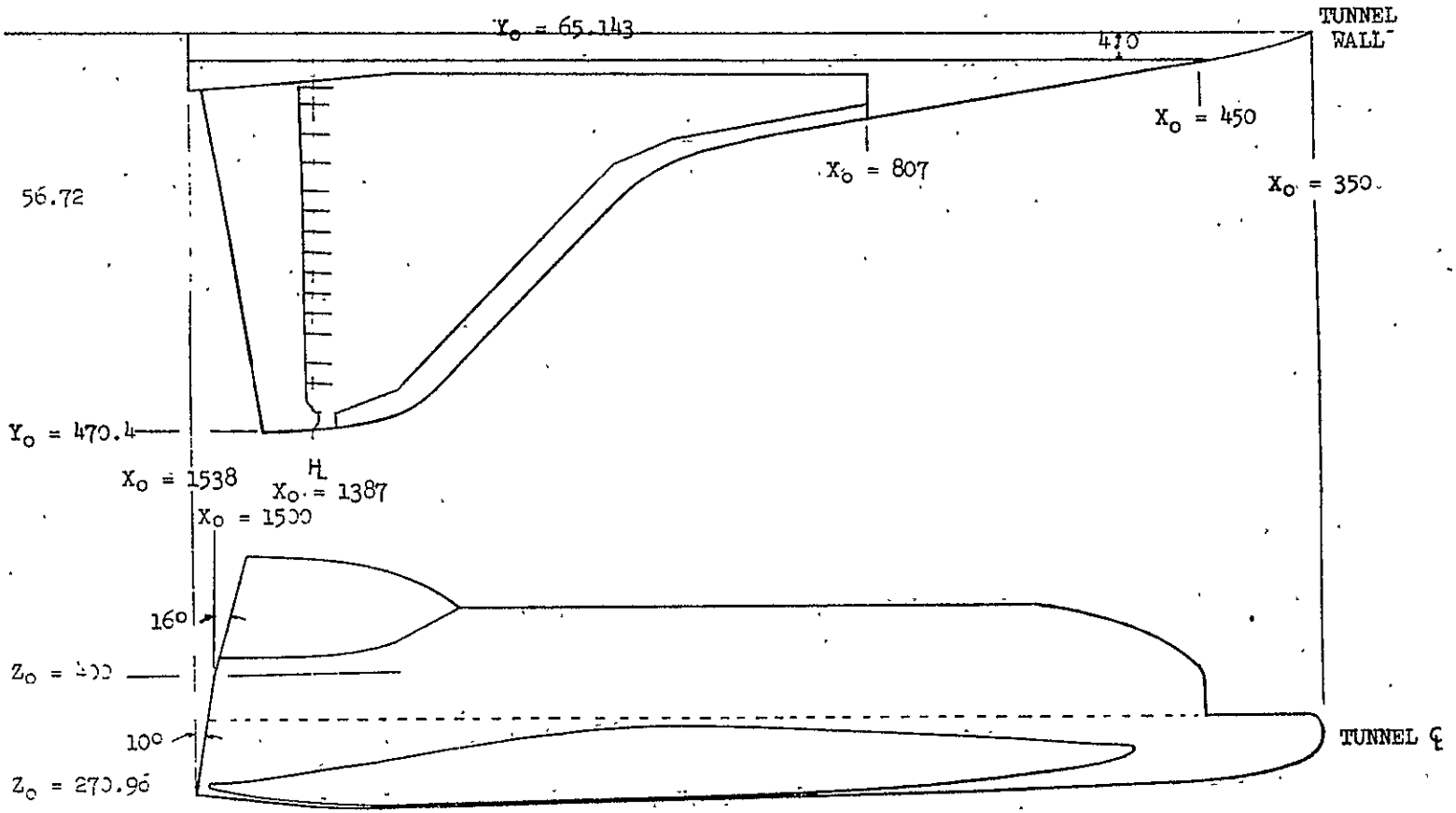

Figure 1. Model installation sketch.

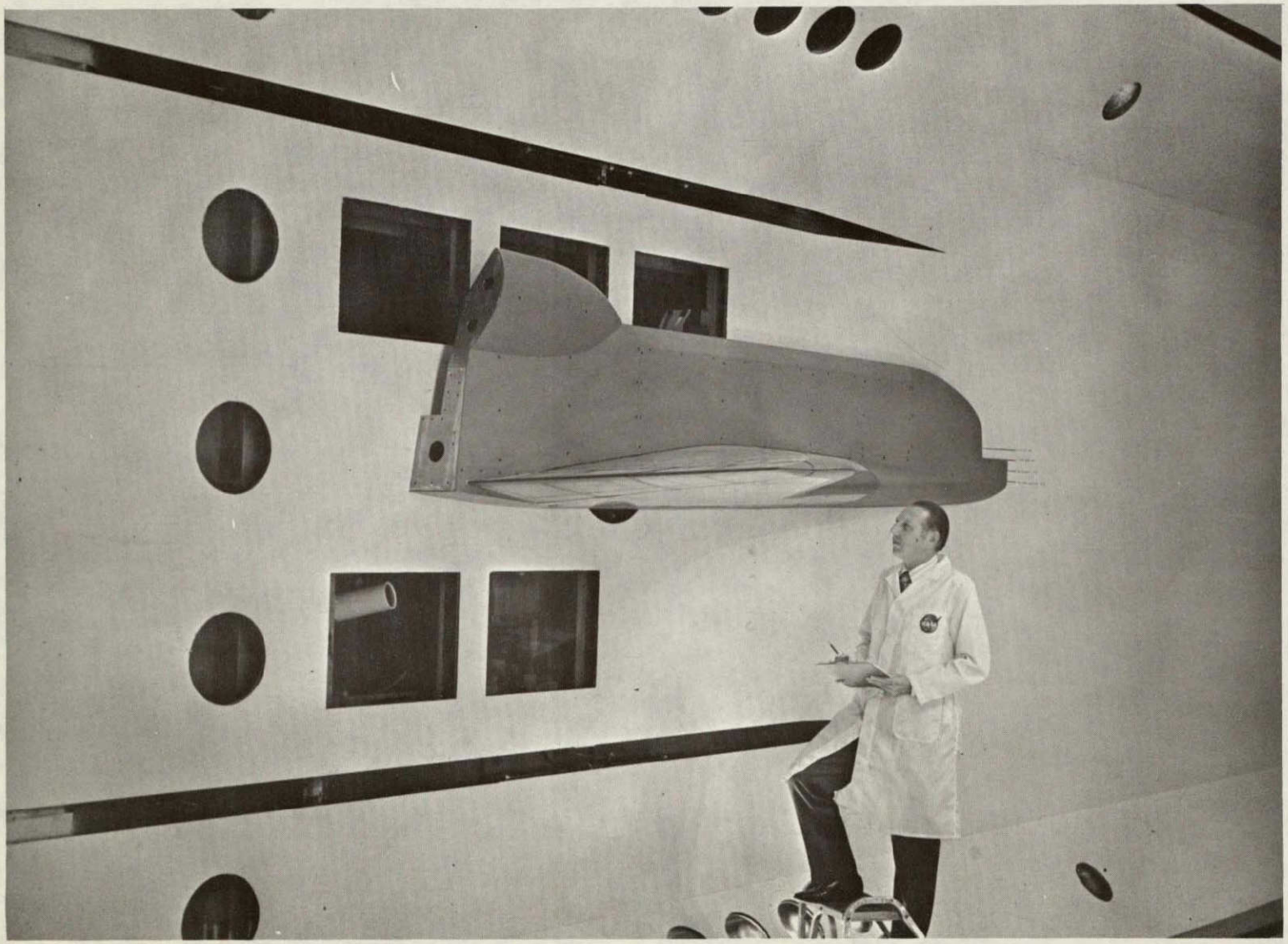

a. Rear Three-quarter View of Model Installation
Figure 2. Model photographs.

b. Front View of Model Installation
Figure 2. Continued.

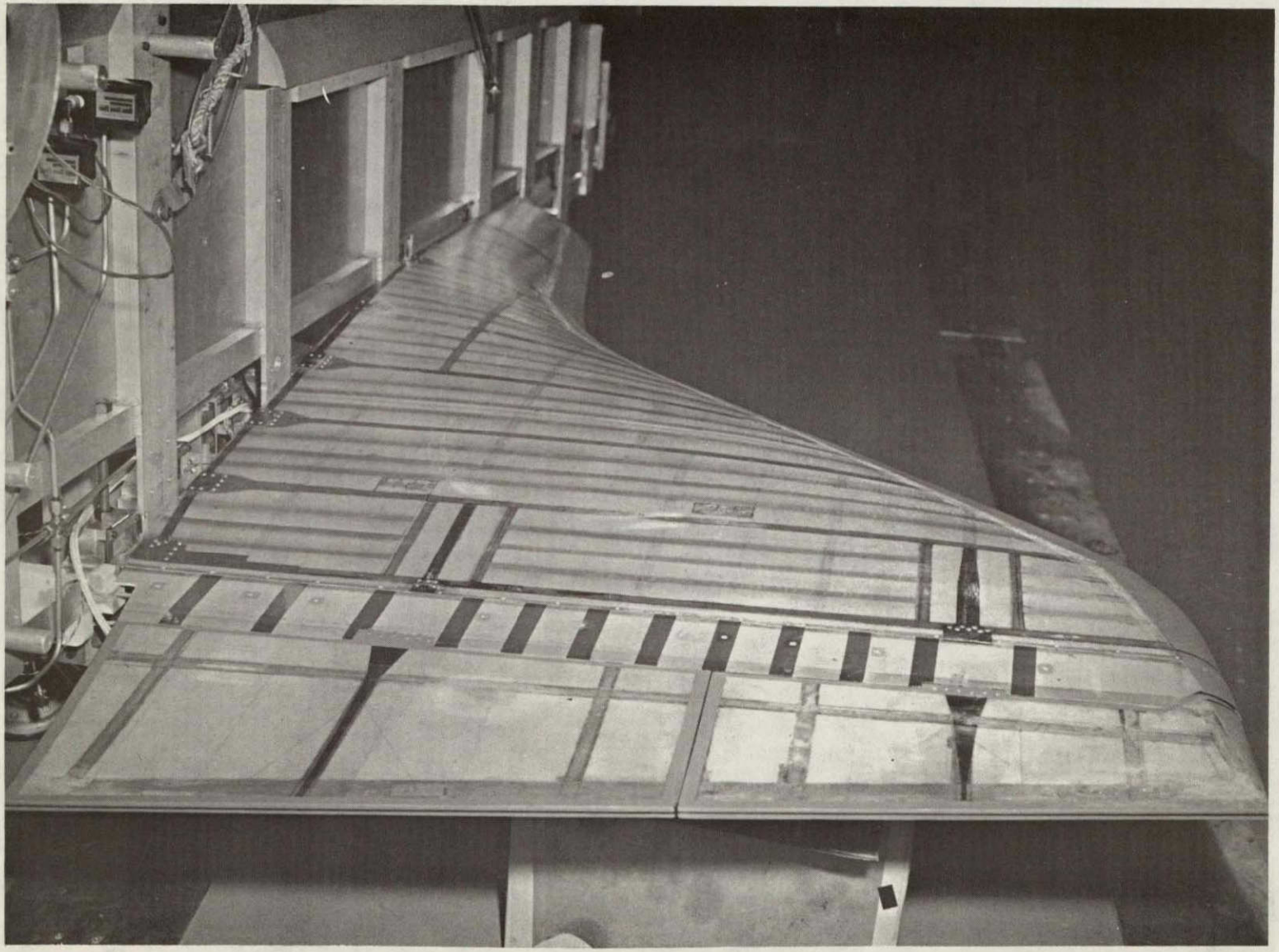

c. Model with Fuselage Skin Removed
Figure 2. Continued.

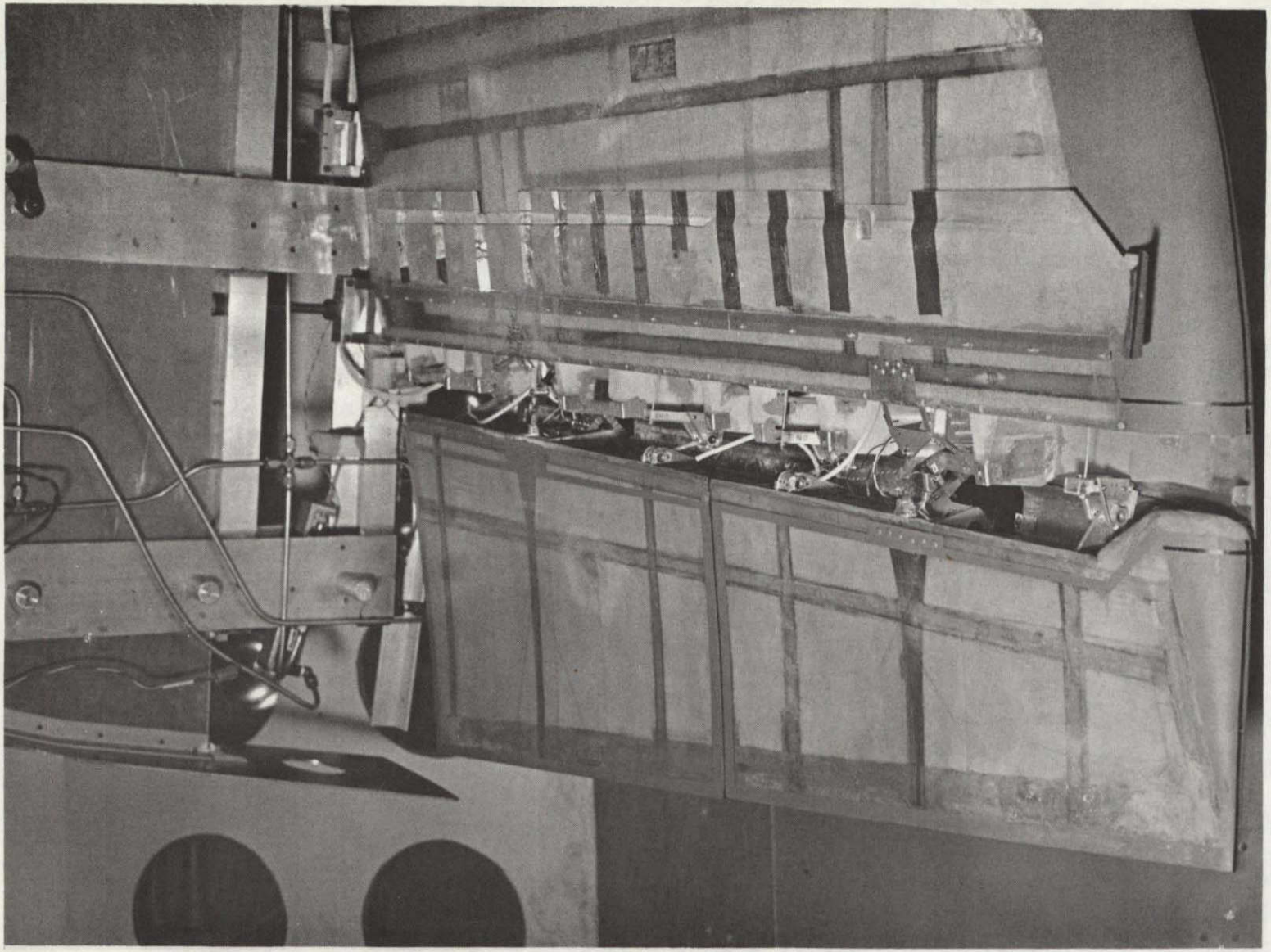

d. Elevon Flexure Arrangement
Figure 2. Concluded.

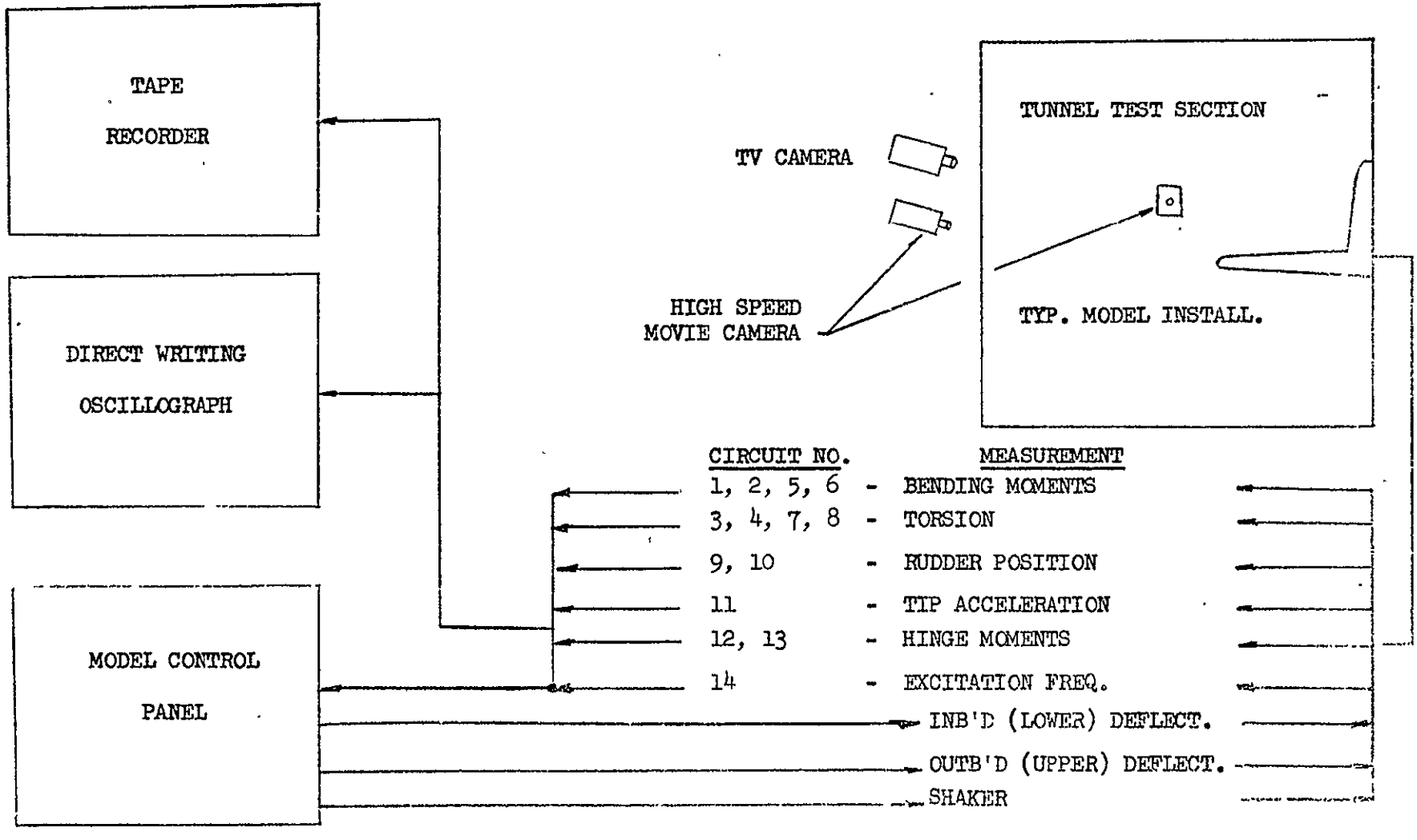

Figure 3. Model instrumentation diagram.

Figure 4. Panel definition for mass and inertia measurements.

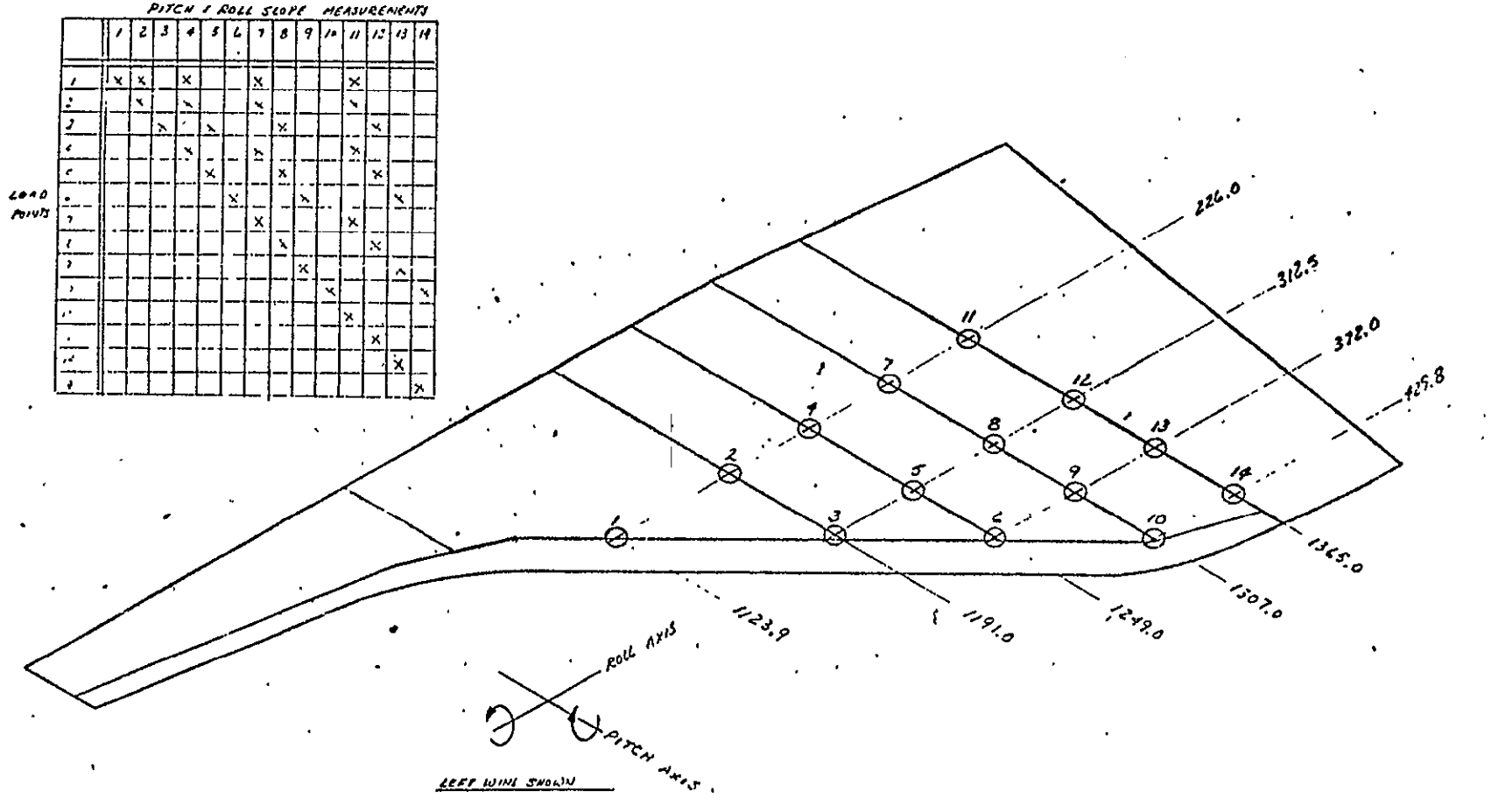

Figure 5. Load points for influence coefficients.

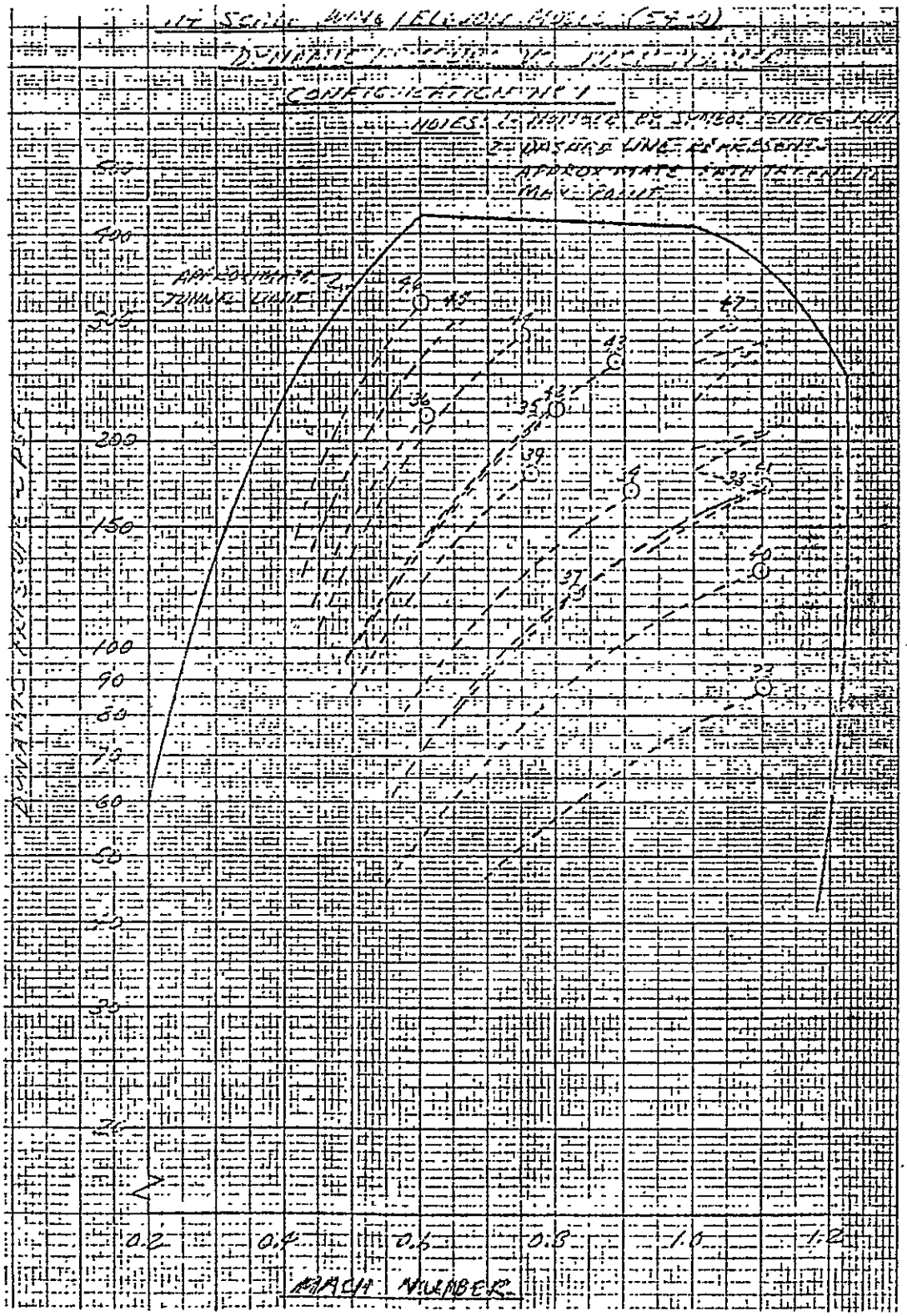

Figure 6. Flutter boundary for Configuration No. 1.

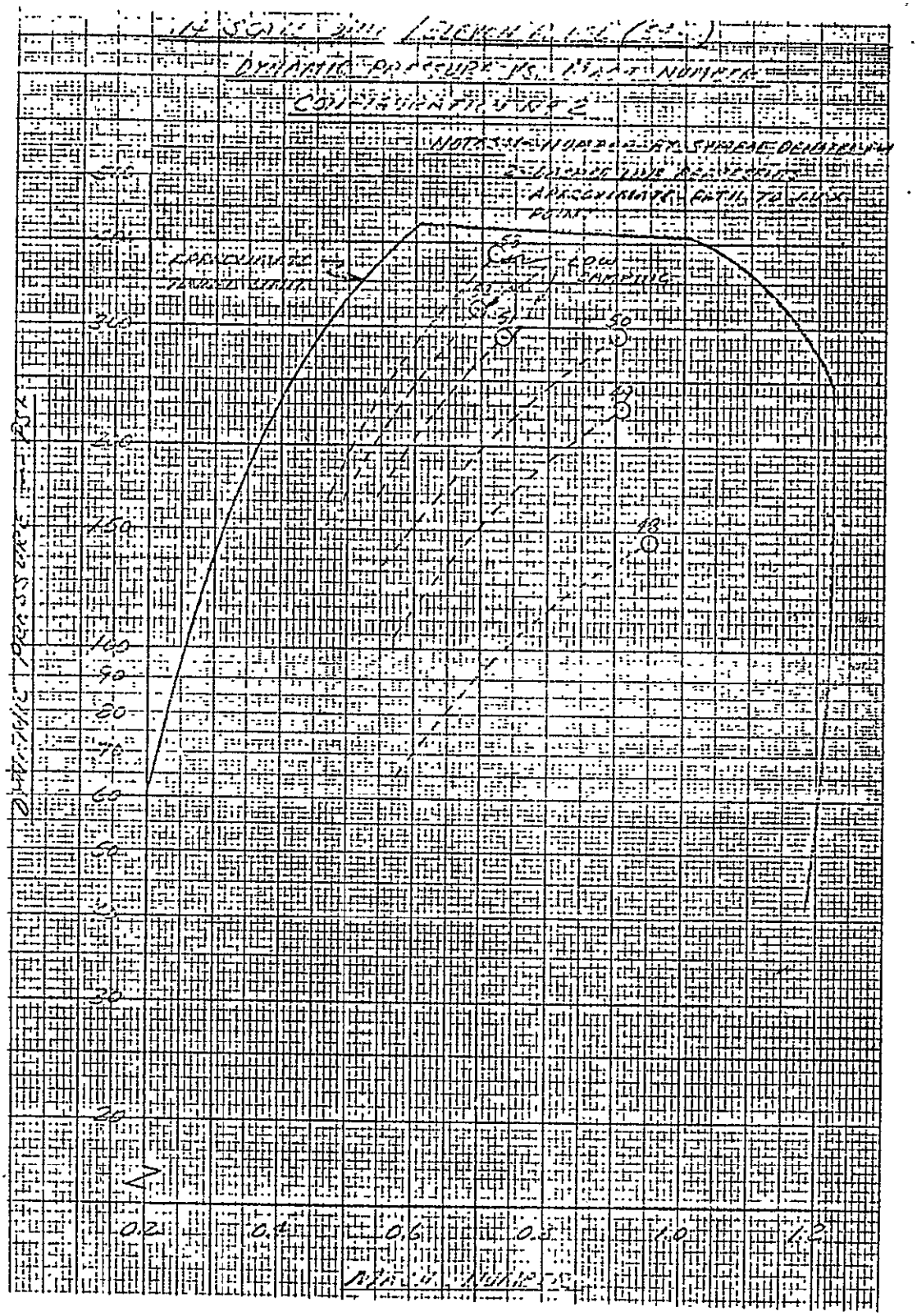

Figure 7. Flutter boundary for Configuration No. 2.

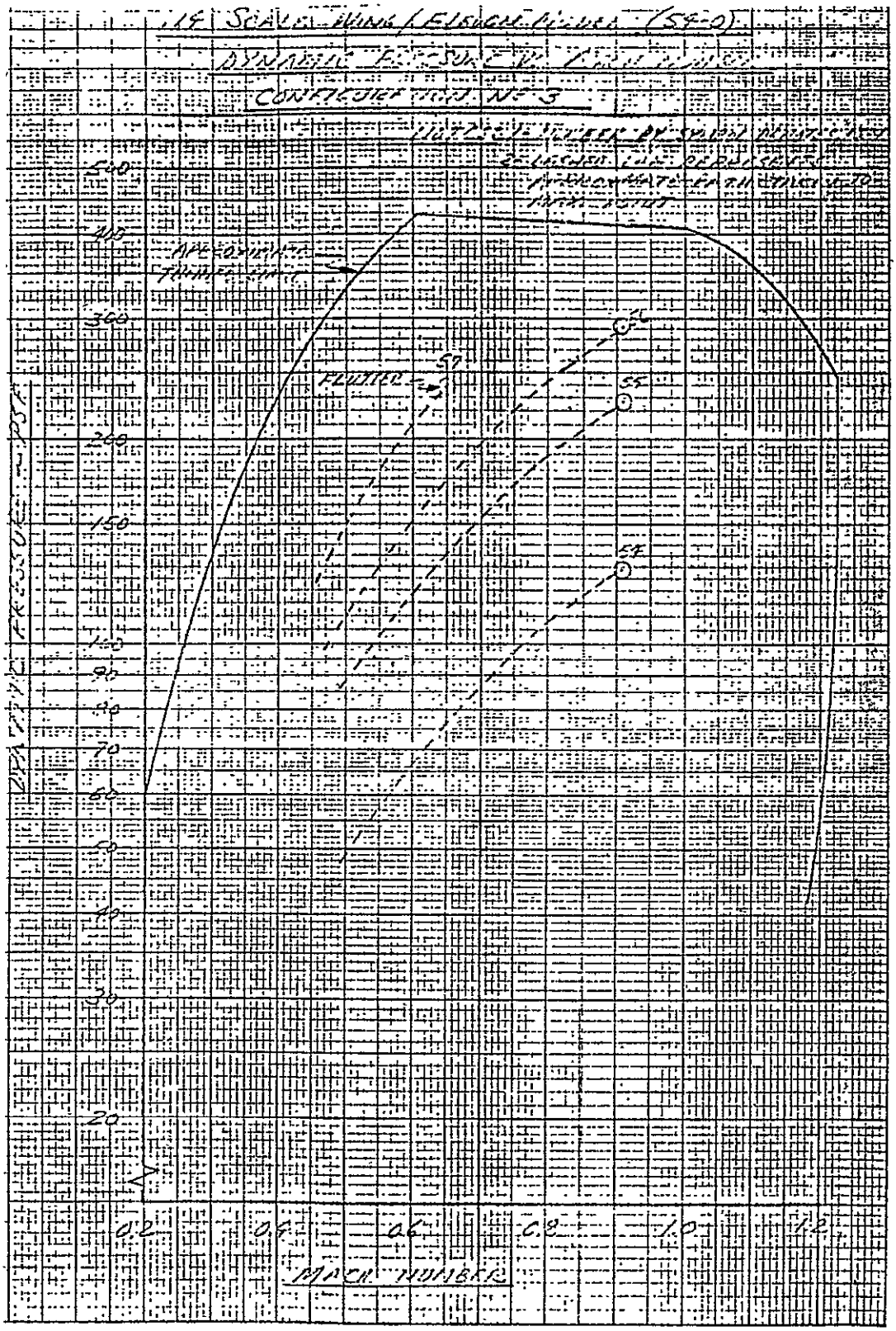

Figure 8. Flutter boundary for Configuration No. 3.

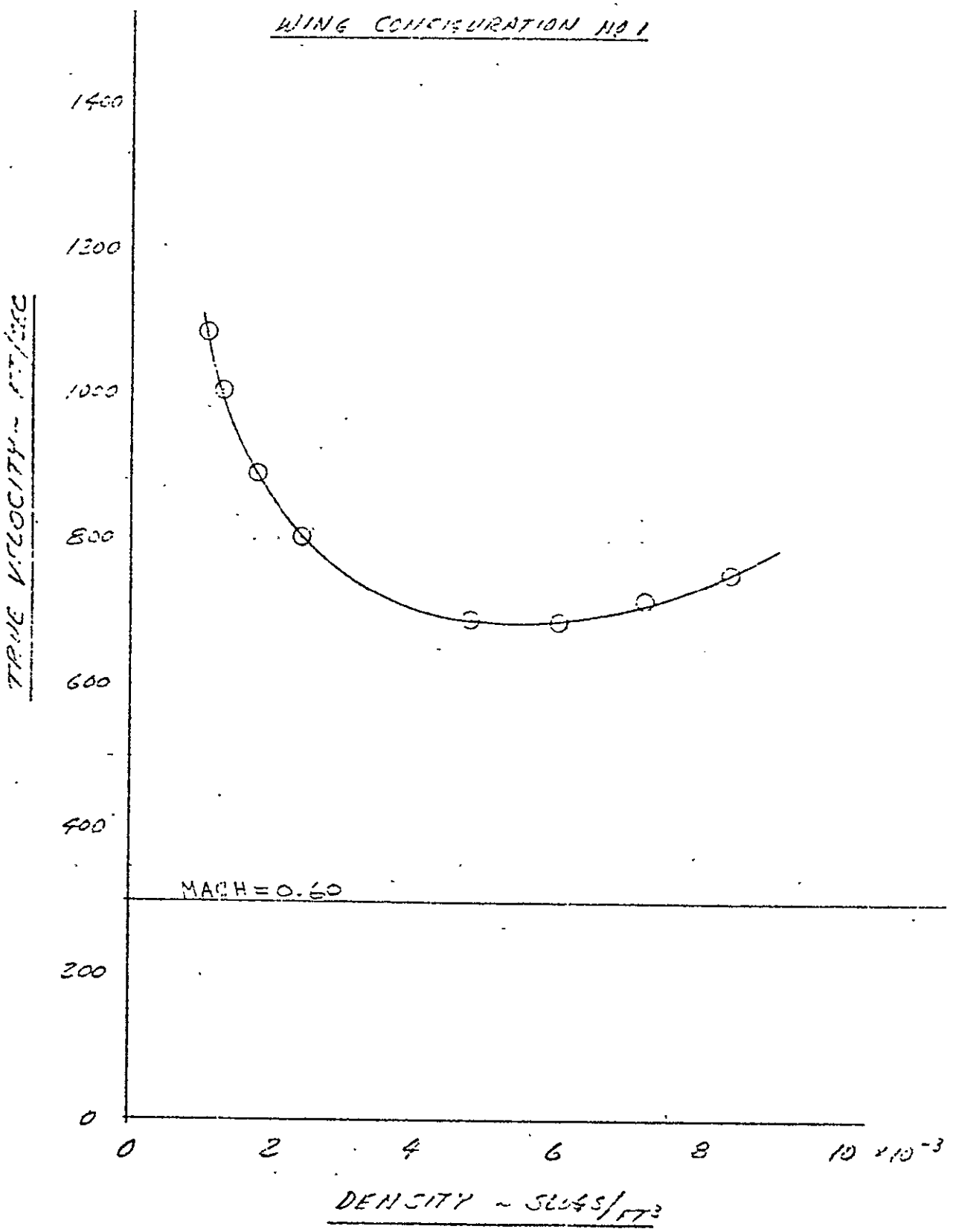

Figure 9. True velocity versus density at Mach .6.

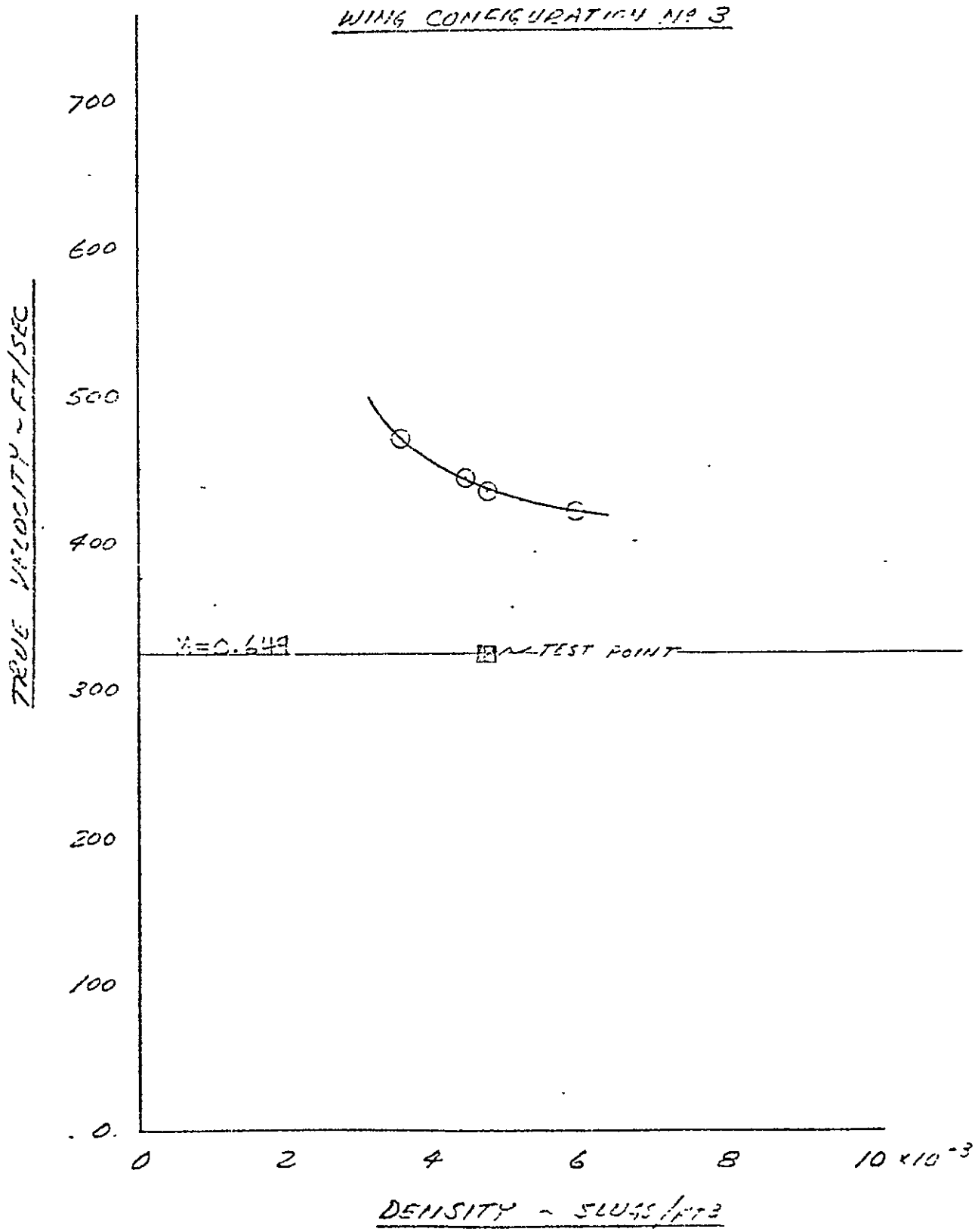

Figure 10. True velocity versus density at Mach .649.

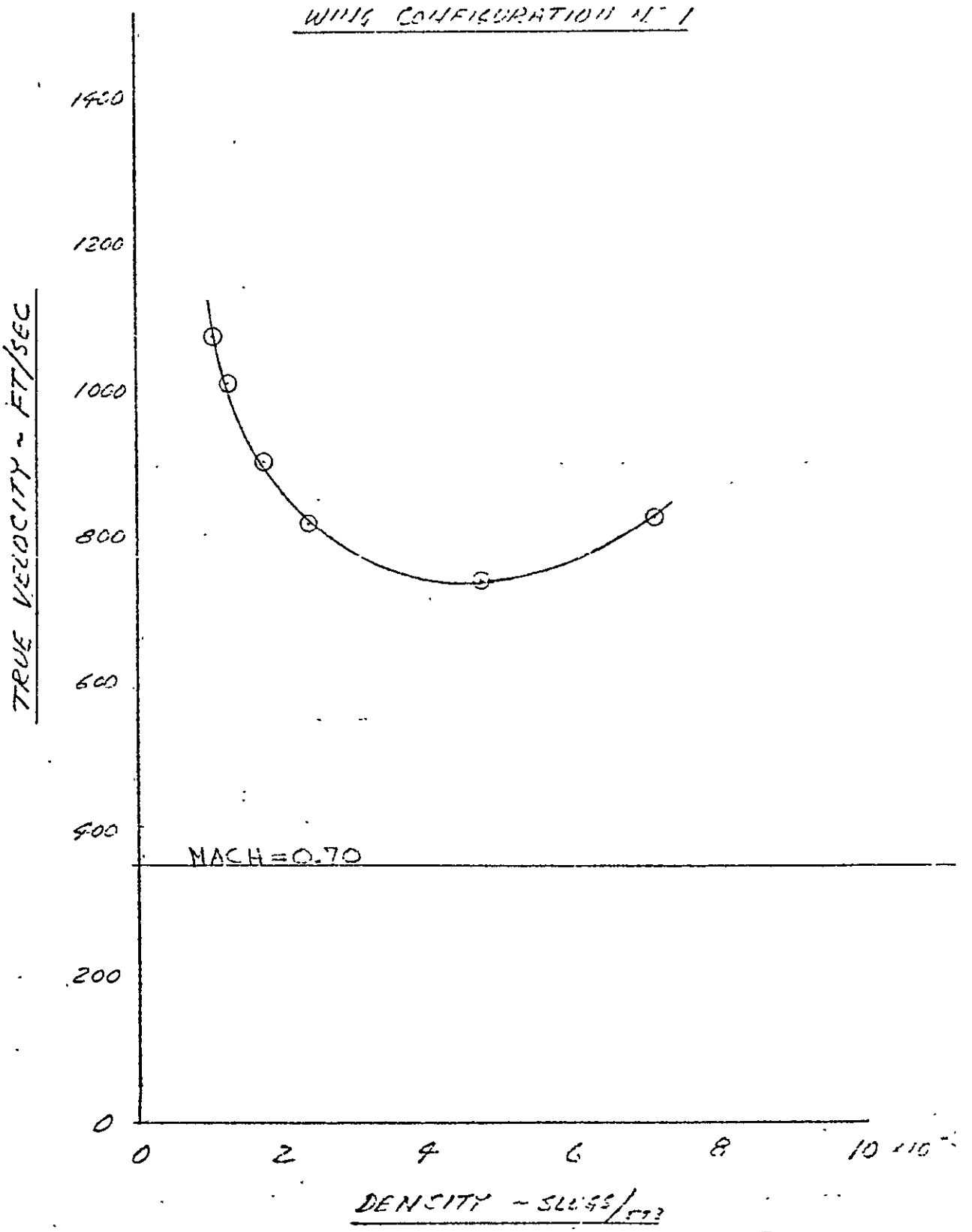

Figure 11. True velocity versus density at Mach .7.

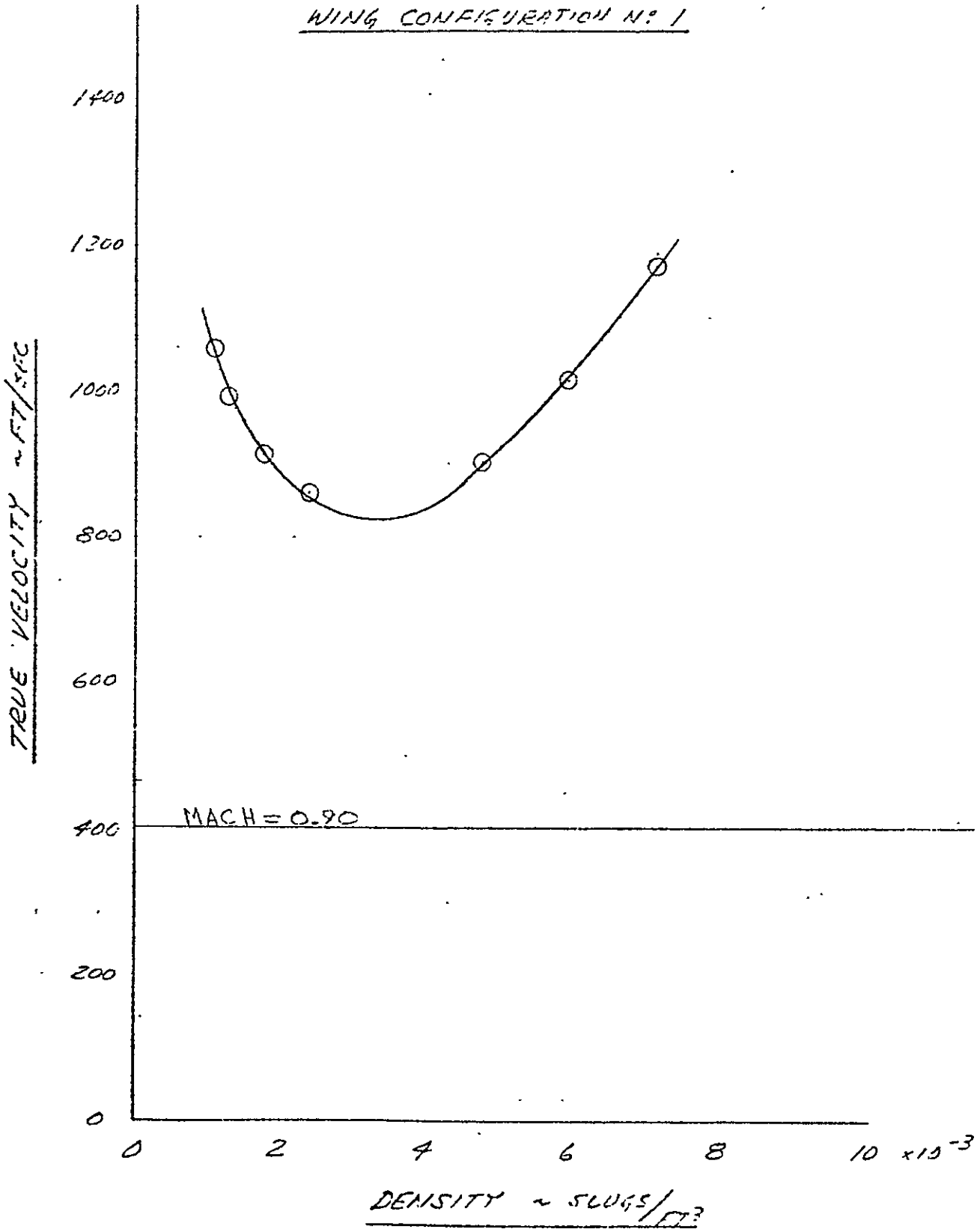

Figure 12. True velocity versus density at Mach .8.

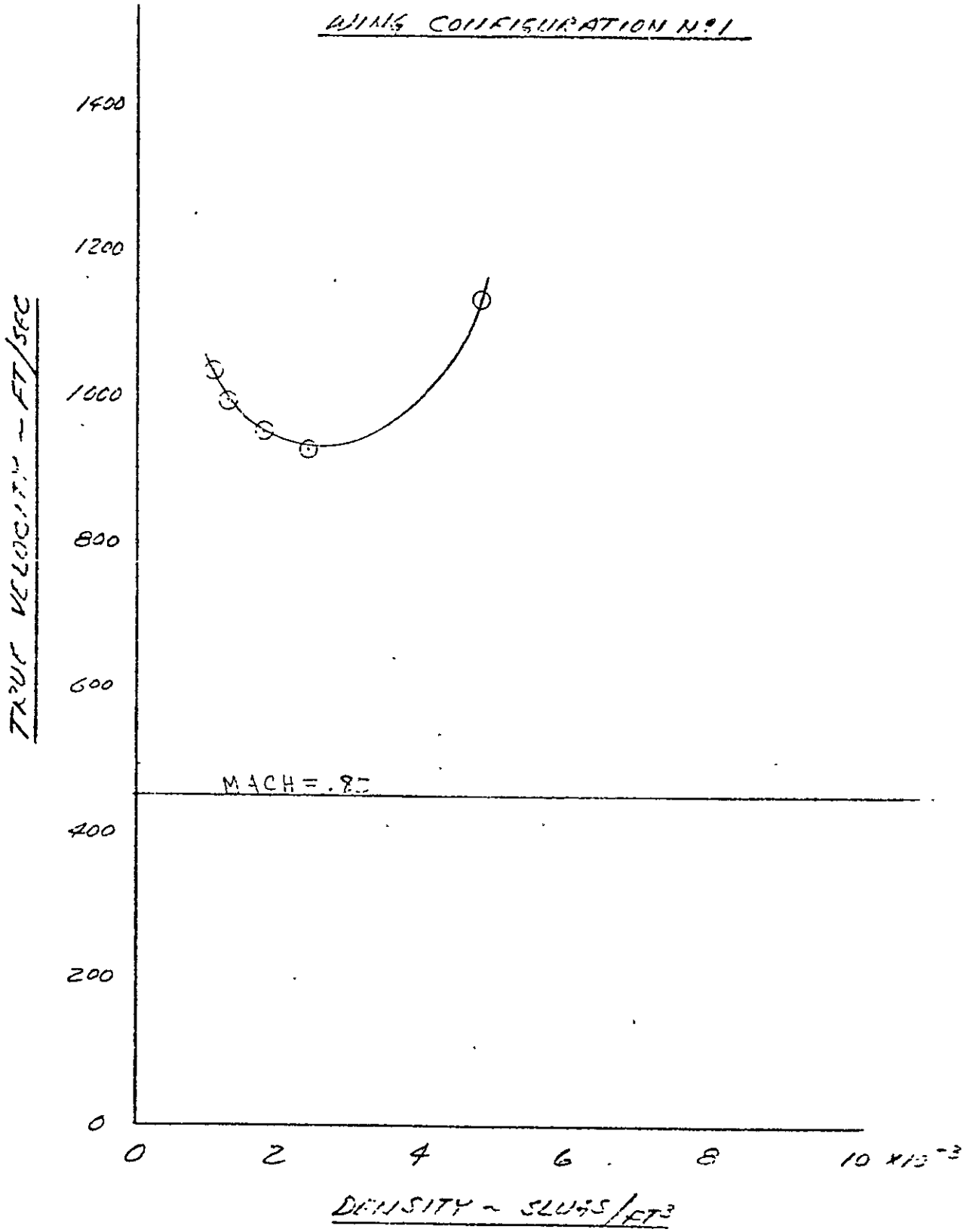

Figure 13. True velocity versus density at Mach .85.

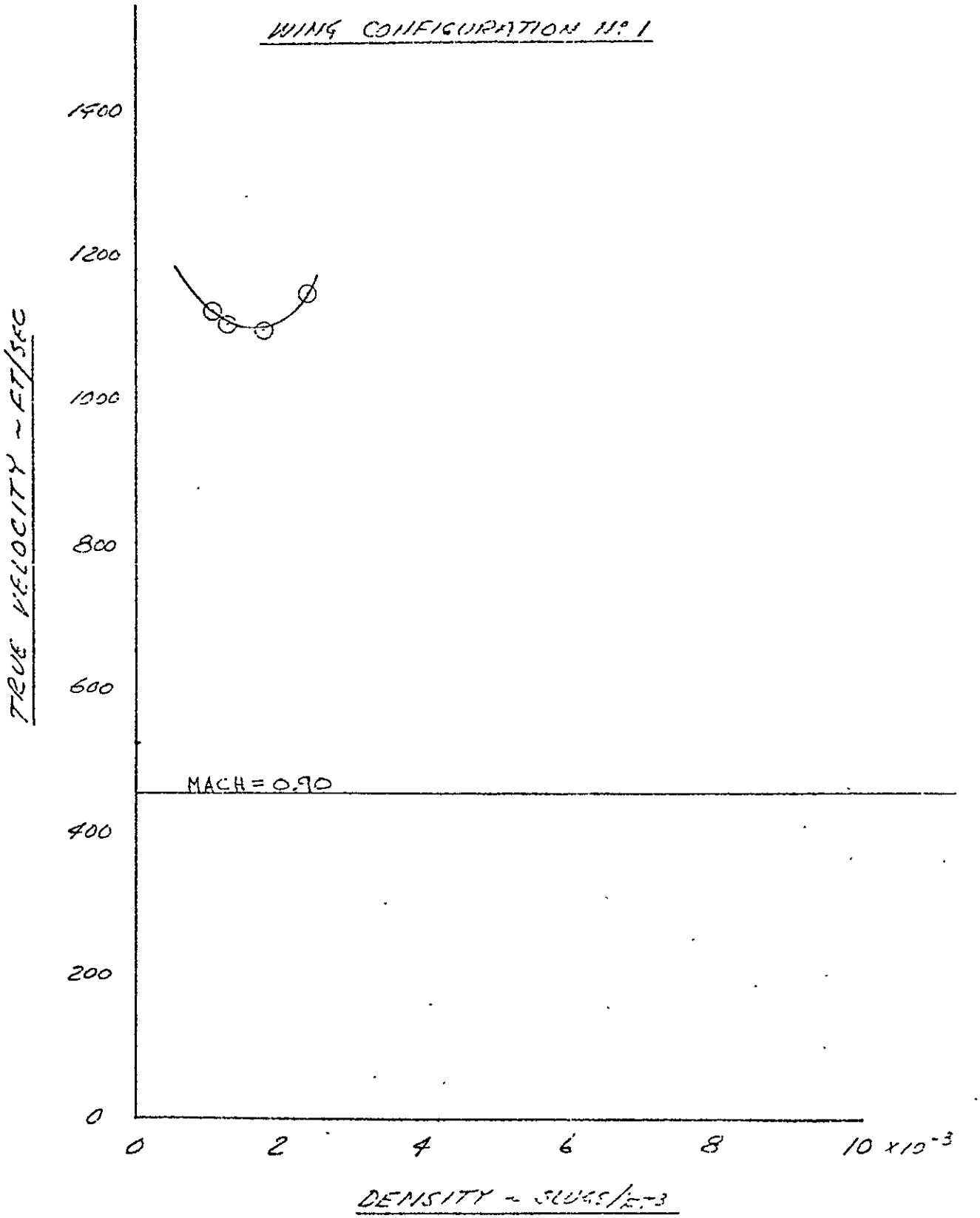

Figure 14. True velocity versus density at Mach .90.

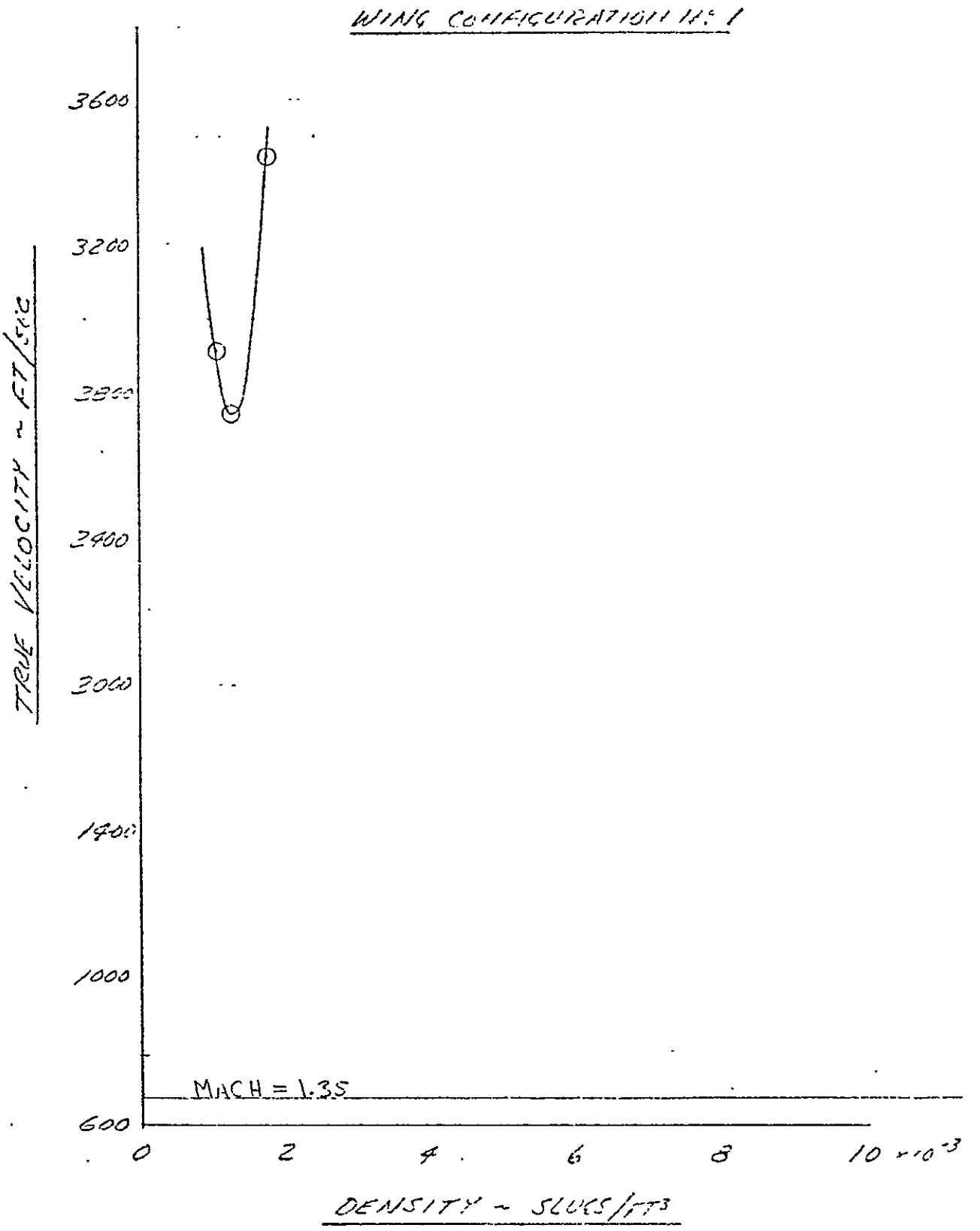

Figure 15. True velocity versus density at Mach 1.35.

Figure 16. Damping versus Mach number.